Hydrogen-Atom Transfer

DOI: 10.1002/anie.201108363

Thermal Hydrogen-Atom Transfer from Methane: The Role of Radicals and Spin States in Oxo-Cluster Chemistry

*Nicolas Dietl, Maria Schlangen, and Helmut Schwarz**

C–H activation · density functional calculations · gas-phase reactions · hydrogen-atom transfer · reaction mechanisms

Dedicated to Harry B. Gray, Joshua Jortner, and Rudolf Zahradník

Hydrogen-atom transfer (HAT), as one of the fundamental reactions in chemistry, is investigated with state-of-the-art gas-phase experiments in conjunction with computational studies. The focus of this Minireview concerns the role that the intrinsic properties of gaseous oxo-clusters play to permit HAT reactivity from saturated hydrocarbons at ambient conditions. In addition, mechanistic implications are discussed which pertain to heterogeneous catalysis. From these combined experimental/computational studies, the crucial role of unpaired spin density at the abstracting atom becomes clear, in distinct contrast to recent conclusions derived from solution-phase experiments.

1. Introduction

> *"The presence of unpaired spin density at the abstracting atom is not a requirement for, or a predictor of, HAT reactivity."*

Challenged by J. M. Mayer's controversial comment[1] on the reaction of a series of hydrocarbons RH with organic radicals and transition-metal complexes, in the following we aim at demonstrating that in gas-phase (ion) chemistry the presence of a spin density at an oxygen atom of various metal and main-group element oxides *is* a requirement for and a predictor of efficient hydrogen-atom transfer (HAT) reactivity at ambient conditions, provided the process is exothermic. After some general considerations of HAT reactions, we will present examples of reactive as well as inert species in terms of HAT reactivity, discuss two mechanistic variants of homolytic C–H bond cleavage, comment on the role of charge states, and address some aspects of heterogeneously catalyzed HAT processes. As a substrate RH, the focus will be on the thermal activation of methane, the most inert of all hydrocarbons.

HAT, which has been regarded[1] as a special class of proton-coupled electron transfer (PCET), plays an important role in a broad range of chemical reactions, covering heterogeneous, homogeneous, and enzymatic reactivity.[2] HAT itself has been characterized both in terms of the timing of the elementary steps and the site of proton and electron transfer as typically described in free-radical chemistry (Figure 1). In contrast, in PCET the actual timing and the location to where H^+ and e^- are transferred might differ; for example, in the homolytic C–H bond scission of saturated and unsaturated hydrocarbons mediated by terminal oxo-ligands in high-valent transition-metal complexes,[3] the electron is accepted by the metal center and the proton transferred to the basic ligand. As to the actual sequence of events, the proton or the electron can be transferred first, and each to a different acceptor orbital. However, this HAT/PCET classification is not rigorously defined, and the assignment becomes less meaningful the smaller the differences between the energies of different HOMOs in the donor or LUMOs in the acceptor are.[2b] In other, more recent studies, the differentiation between HAT and PCET has been described in terms of an electronically adiabatic and a non-adiabatic proton transfer, respectively.[4]

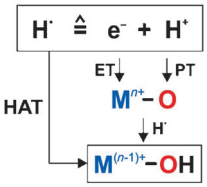

Figure 1. Schematic description of HAT versus proton-coupled electron transfer

[*] Dipl.-Chem. N. Dietl, Dr. M. Schlangen, Prof. Dr. H. Schwarz
Institut für Chemie, Technische Universität Berlin
Strasse des 17. Juni 135, 10623 Berlin (Germany)
E-mail: helmut.schwarz@mail.chem.tu-berlin.de
Prof. Dr. H. Schwarz
Chemistry Department, Faculty of Science
King Abdulaziz University, Jeddah 21589 (Saudi Arabia)
E-mail: hschwarz@kau.edu.sa

Mayer's conclusion[1] is based on a Polanyi correlation,[5] that is, a correlation between $\log k$ and ΔH,[6] for the reactions of a particular substrate with different oxidants including oxyl radicals with doublet spin states, an $S = 5/2$ iron (III) complex, antiferromagnetically coupled Mn dimers, as well as diamagnetic (d^0) permanganate $[MnO_4]^-$,[1,2c,7] and cleavage of the C–H bond is assumed as the rate-determining step for all systems investigated. Further, Marcus theory—originally developed for electron-transfer processes[8]—has been applied, and the Polanyi correlation has then been analyzed using self-exchange rate constants which have been measured for the individual systems to estimate the intrinsic barrier of the Marcus equation. Thus, this intrinsic barrier of the Marcus equation for a HAT reaction $R'H + R^{\bullet} \rightarrow R'^{\bullet} + RH$ can be determined by the barriers for the self-exchange reactions $RH + R^{\bullet} \rightarrow R^{\bullet} + RH$ and $R'H + R'^{\bullet} \rightarrow R'^{\bullet} + R'H$ having no thermodynamic driving force ($\Delta G = 0$), and it corresponds to the reorganization energies of the reactants to accept and donate the hydrogen atom, respectively.[1,7b] The need to generate a so-called "prepared state" has already been discussed at great length in the analysis of many organic reactions, using valence bond (VB) theory.[9] If the reacting substrate is not prepared for the bonding changes in the course of the reaction, higher activation barriers will result. Consequently, the smallest intrinsic barrier is expected for those reactants that do not need to rearrange to a substantial degree to accept or donate the hydrogen atom, respectively. This requirement is fulfilled for complexes with oxygen-centered radicals which already have the ideal properties to accept $H^{\bullet}$, and are thus *prepared* to undergo efficient HAT reactions. Of course, with substrates which have rather weak C–H bonds, hydrogen atoms may be extracted by non-radical reagents, however, in these cases energy is nevertheless necessary to access a suitable electronic structure to form a bond to the incoming hydrogen atom. For example, it has been shown by detailed DFT calculations that an oxyl-radical character of the Mn=O group of a manganese porphyrin complex is necessary for the efficient C–H bond cleavage; this requirement is not provided by the unreactive singlet ground state.[10] Further, VB modeling for the reaction of CrO_2Cl_2 with alkanes in solution revealed that the bonding pair of the closed-shell reactant, that is, two electrons of the Cr=O bond, must be decoupled prior to the reaction for it to exhibit HAT reactivity.[9] Also the much smaller, seemingly simple system of the gas-phase couple $[CuO]^+/CH_4$,[11] in which the spin states of $[CuO]^+$ control the chemoselectivity of C–H bond activation is a recent, even more striking example, demonstrating the importance of oxygen-centered radicals for HAT reactions. In fact, many observations gathered in the last decades in gas-phase (ion) chemistry support the conjecture of the importance of a radical site for the efficient, thermal activation of methane, which is the most inert and challenging substrate.[12] As verified by state-of-the-art quantum chemical calculations, all of the numerous examples of HAT from methane observed in gas-phase experiments are achieved by metal or non-metal oxide species which have a high spin density at an oxygen atom to which the hydrogen is transferred; they include $[V_xP_{4-x}O_{10}]^{\bullet+}$ ($x = 0$, 2–4),[13] $[(Al_2O_3)_x]^{\bullet+}$ ($x = 3$–5),[14] $[FeO]^{\bullet+}$,[15] $[VAlO_4]^{\bullet+}$,[16] and others. Furthermore, oxide species lacking this property are not reactive or only activate much weaker C–H bonds of, for example, higher alkanes or those at allylic, benzylic, or otherwise activated positions. A comparison of the cationic dioxides $[MO_2]^+$ (M = Ti, V, Zr, Nb) may serve as an instructive example.[17] The ionization of TiO_2 and ZrO_2 corresponds to the removal of an electron from the strong M=O bond leaving an unpaired electron at the oxygen in cationic $[TiO_2]^{\bullet+}$ and $[ZrO_2]^{\bullet+}$; both dioxides are capable of HAT from methane at ambient conditions. In contrast, the *closed-shell*, singlet species $[VO_2]^+$ and $[NbO_2]^+$ are unreactive with regard to the C–H bond activation of methane. A similar reasoning holds true for $[MoO_x]^{\bullet+}$ ($x = 2, 3$);[18] while two strong Mo=O bonds (bond dissociation energy (BDE) = 542 kJ mol^{-1}) are present in $[MoO_2]^{\bullet+}$ with the additional electron being located at the metal, the bonding situation of $[MoO_3]^{\bullet+}$ allows the formation of only two Mo=O bonds and one weak M–O$^{\bullet}$ bond (BDE = 257 kJ mol^{-1}). Accordingly, $[MoO_3]^{\bullet+}$ is capable of hydrogen-atom abstraction from methane, while $[MoO_2]^{\bullet+}$ is inert under these conditions.[18] Also in comparative studies of polynuclear oxide species which are composed of the same elements with the only difference being the presence or absence of M–O$^{\bullet}$ radicals, those with the radicals a much higher reactivity towards methane; examples of aluminum-

Nicolas Dietl studied chemistry at the Technische Universität Berlin (Germany) and at the ETH Zürich (Switzerland). After conducting his Diploma thesis under the supervision of Prof. Helmut Schwarz in 2009, he stayed in the group for his Ph.D. studies. His current research deals with mass-spectrometric and computational studies on gaseous oxide clusters as model systems for C–H bond activation and catalytic oxidation processes.

Maria Schlangen studied chemistry at the University of Cologne (1999–2000) and at the Technische Universität Berlin (2000–2004). She received her Ph.D. with Professor Helmut Schwarz in 2008, dealing with reactivity studies on gaseous nickel complexes. Since December 2007 Dr. Schlangen is in charge of the mass-spectrometry facility of the Institute of Chemistry at the Technische Universität Berlin.

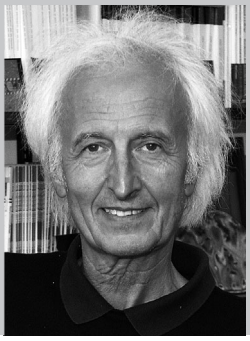

Helmut Schwarz has been Professor of Chemistry at the Technische Universität Berlin as since 1978. In January 2008 he took up the presidency of the Alexander von Humboldt Foundation. Dr. Schwarz has occupied visiting positions at 14 academic institutions worldwide and has delivered more than 900 invited or name lectures.

containing oxide clusters will be discussed in more detail in Section 3.2.

2. HAT in the Gas Phase: Two Mechanistic Scenarios

Regarding the mechanistic details of the HAT process, two variants of gas-phase hydrogen-atom abstraction by oxo-species have been reported. The first one corresponds to a direct HAT pathway from the hydrocarbon to the abstracting oxygen atom; the second mode involves several steps including a metal-mediated activation step for which an empty coordination site at the metal atom is required. Numerous examples are known for either scenario, and details of the two variants are presented in the following.

The direct HAT process prevails predominantly for *open-shell* oxide clusters mostly with metal centers in relatively high oxidation states and with coordination numbers that prevent the indirect pathway from occurring. Examples showing this pattern include the non-metal system $[SO_2]^{\bullet+}$,[19] as well as metal containing clusters $[Ce_2O_4]^{\bullet+}$,[20] $[V_xP_{4-x}O_{10}]^{\bullet+}$ $(x=0,2\text{–}4)$,[13] $[(Al_2O_3)_x]^{\bullet+}$ $(x=3\text{–}5)$,[14] $[VIO_4]^{\bullet+}$,[16] or $[(V_2O_5)_x(SiO_2)_y]^{\bullet+}$ $(x=1,\ 2;\ y=1\text{–}4)$.[21] The polynuclear oxide cluster $[V_4O_{10}]^{\bullet+}$ was studied at great length to reveal the mechanistic features of the direct HAT process.[13a] It has been shown that the reaction proceeds barrier-free, without the formation of a long-lived encounter complex $[V_4O_{10}]^{\bullet+}\cdots CH_4$, directly to the intermediate $[V_4O_9OH]^{+}\cdots CH_3^{\bullet}$; in this intermediate the methyl group is loosely coordinated to the hydrogen atom of the newly formed hydroxy group. The rather exothermic reaction is completed by loss of the $CH_3^{\bullet}$ radical, resulting in the formation of $[V_4O_9(OH)]^{+}$. The absence of any barrier along the reaction pathway is consistent with the high reaction efficiency of 60% relative to the collision rate ($k=5.5\times10^{-10}\,cm^3\,s^{-1}\,molecule^{-1}$).[13a] Finally, HAT from the $[V_4O_{10}]^{\bullet+}/CH_2D_2$ couple is associated with a small intramolecular kinetic isotope effect (KIE) of 1.35. In addition to the experimental results, detailed molecular dynamics (MD) simulations provide further evidence for a fast and barrier-free HAT pathway (Figure 2). According to the simulations, the potential energy decreases continuously in the first 450 fs owing to the attractive forces between the incoming neutral methane and the ionic cluster; once more, no barrier has been located. Simultaneously, the O–H (Figure 2; red line) and V–C (green line) separation shrink steadily, while the C–H distance (blue line) slowly increases. After 450 fs, the system has lost approximately 102 kJ mol^{-1} of potential energy which is then channeled into the C–H and O–H stretching modes resulting in the oscillations of the hydrogen atom between the vanadyl oxygen and the methyl carbon atoms. Further, the V–C distance decreases until $t=470$ fs, then it slowly increases, thus indicating the beginning of the expulsion of the $CH_3^{\bullet}$ radical; this step is completed only after significantly longer simulation times.

The indirect, metal-mediated pathway is generally limited to small, mostly diatomic metal oxides, such as $[MnO]^{\bullet+}$,[22] $[FeO]^{\bullet+}$,[15] $[MgO]^{\bullet+}$,[23] $[PbO]^{\bullet+}$,[24] $[CuO]^{+}$,[11] $[SnO]^{\bullet+}$,[25] or

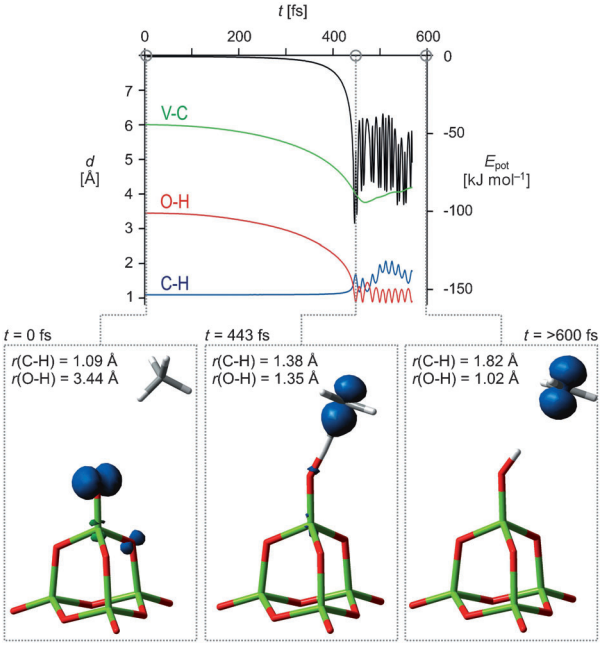

Figure 2. MD simulation showing the evolution of the potential energy and the relevant bond lengths (green V, red O) for the thermal reaction of $[V_4O_{10}]^{\bullet+}$ with methane. The energy is shown in black [kJ mol^{-1}], d(C–H) in blue, d(O–H) in red, and d(V–C) in green. The fluctuations after 450 fs result from vibrational motions, mainly of the OH group. The blue isosurface indicates the spin density within the respective intermediate (adapted from Ref. [13a]).

$[GeO]^{\bullet+}$.[25] These systems have a vacant coordination site at the metal atom; thus, an encounter complex $[CH_4\cdots M{-}O^{\bullet}]^{+}$ and an intermediate $[CH_3^{\bullet}\cdots M{-}OH]^{+}$ are generated in the course of the reaction path. The $[MgO]^{\bullet+}/CH_4$ couple may serve as a good example without being further complicated by more complex reactivity scenarios, for example, two-state reactivity[26] which occurs with $[FeO]^{\bullet+}$ or $[CuO]^{\bullet+}$, for example. The simplified potential energy surface is shown in Figure 3. The initially generated adduct complex has gained enough internal energy for the hydrocarbon to migrate around the metal center towards the reactive oxo site at which the C–H bond fission occurs. Subsequently, the newly formed methyl group, in a metal-controlled fashion, returns back to give the linear intermediate $[CH_3^{\bullet}\cdots M{-}OH]^{+}$; this intermediate represents a complex between a protonated magnesium-oxide unit and a loosely bound methyl radical which now carries more than 98% of the spin. The overall exothermic reaction is completed by loss of a $CH_3^{\bullet}$ radical from this intermediate. While the alternative rebound mechanism to generate methanol is thermochemically even more favorable than HAT, it is kinetically and entropically less attractive.

Contrary to the direct hydrogen-atom abstraction from CH_4, which is generally characterized by rather small KIEs, metal-mediated homolytic C–H bond cleavages exhibit larger KIEs, typically greater than 2.0. Further, it has been noted that there is, for a given reaction type, a relationship between the size of the KIEs and the overall rate coefficients of the hydrogen-atom abstraction from methane.[27] For example, the intermolecular KIEs, derived from the reactions of

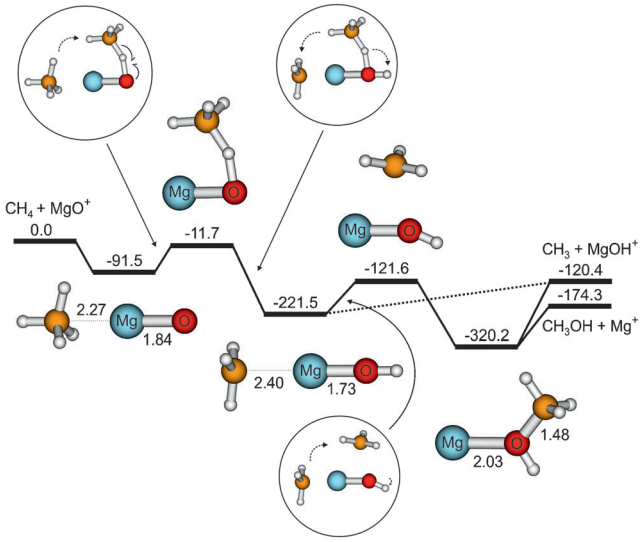

Figure 3. Potential-energy surface [kJ mol^{-1}] for the reaction of $MgO^{\bullet+}$ with CH_4 calculated at the MP2/6-311+G(2d,2p) level of theory; selected bond lengths [Å]. The encircled structures depict the rearrangements occurring along the reaction coordinate (adapted from Ref. [23]).

various diatomic $[MO]^{\bullet+}$ species with CH_4 and CD_4, increase from about 1.3 for $[MgO]^{\bullet+}$, to 2.1 and 2.4 for $[CaO]^{\bullet+}$ and $[SrO]^{\bullet+}$, respectively, to 3.2 for $[BaO]^{\bullet+}$.[27,28] This trend of increasing KIEs is paralleled with a decrease of the overall rate coefficients for the activation of methane, from 3.9×10^{-10} cm^3 s^{-1} molecule^{-1} for $[MgO]^{\bullet+}$ and 2.9×10^{-10} for $[CaO]^{\bullet+}$ to 9.8×10^{-11} and 1.1×10^{-11} for $[SrO]^{\bullet+}$ and $[BaO]^{\bullet+}$, respectively, thus, reflecting an increasingly late transition state (TS) and thereby an increasing KIE. With regard to catalysis, this observation implies that the less-reactive oxidants exhibit higher selectivities in terms of the associated KIEs, apparently in line with the time-honored Bell–Evans–Polanyi principle.[5,29]

3. HAT in the Gas Phase and the Role of Oxygen-Centered Radicals

3.1. Heteronuclear Oxide Clusters: The Question about the Reactive Site

From surface studies it was conjectured that (structurally often ill-defined) non-metal species, for example, phosphates or silicates, work as catalytically innocent linkers between the active metal oxide sites;[30] well-known examples are the so-called VPO-catalysts, permitting the large-scale transformation of *n*-butane to maleic anhydride.[31] In 2009, this assumption was questioned by gas-phase studies on metal-free *open-shell* oxide cations, that is, $[SO_2]^{\bullet+}$ and $[P_4O_{10}]^{\bullet+}$, which efficiently activate methane at ambient conditions.[13b,19] Similar to $[V_4O_{10}]^{\bullet+}$, UB3LYP-based computations assign to the most stable isomer of the $[P_4O_{10}]^{\bullet+}$ cluster ion a slightly Jahn–Teller distorted tetrahedral cage structure with C_s symmetry. In comparison with neutral P_4O_{10}, one of the terminal P–O bonds in $[P_4O_{10}]^{\bullet+}$ is elongated from 1.46 to 1.57 Å because of the removal of an electron from the P=O bond, and 88% of the spin is localized at this terminal oxygen atom. Moreover, $[P_4O_{10}]^{\bullet+}$ is even slightly more reactive than the metallic analogue $[V_4O_{10}]^{\bullet+}$ with respect to the homolytic C–H bond fission of methane ($k=6.4\times10^{-10}$ cm^3 s^{-1} molecule^{-1} ($\phi=66\%$) vs. $k=5.5\times10^{-10}$ cm^3 s^{-1} molecule^{-1} ($\phi=60\%$), respectively). In addition, according to DFT calculations the barrier-free HAT process is associated with a total gain of energy of 115 kJ mol^{-1}; hence about 28 kJ mol^{-1} more exothermic than for $[V_4O_{10}]^{\bullet+}$ (Figure 4). These results have been verified by more accurate ab initio methods using the CCSD(T) level of theory.[13b]

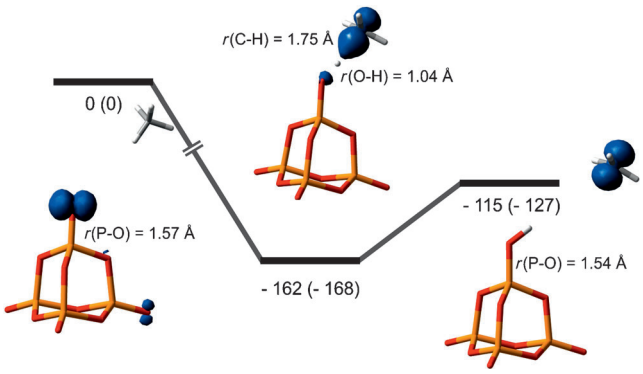

Figure 4. Potential-energy surface for the reaction of $[P_4O_{10}]^{\bullet+}$ with CH_4 (yellow P, red O); the relative energies from DFT and CCSD(T) (in parentheses) are corrected for zero-point energy and given in kJ mol^{-1}. Selected bond lengths are given in Å and the blue isosurface indicates the spin density.

The higher HAT reactivity of $[P_4O_{10}]^{\bullet+}$ is further illustrated by a comparison of the reactions with ethene: while $[P_4O_{10}]^{\bullet+}$ abstracts a hydrogen atom also from C_2H_4 to generate the *closed-shell* cluster $[P_4O_9OH]^+$,[32] $[V_4O_{10}]^{\bullet+}$ does not engage in HAT but gives exclusively rise to an oxygen-atom transfer (OAT) to this hydrocarbon.[33] To learn more about the role of the metal and/or non-metal atoms of the reactive oxide species, various ionic as well as neutral, heteronuclear oxo-clusters were studied with respect to their electronic structures and reactivities, including $[V_xAl_yO_z]^{+/-}$ ($x+y=2,\ 3,\ 4;\ z=3$–10),[16,34] $[(V_2O_5)_x(SiO_2)_y]^{+/-}$ ($x=1,\ 2;\ y=1$–4),[21,35] $[V_{4-x}Y_xO_{10-x}]^{\bullet+}$ ($x=1,2$),[36] $[V_xP_{4-x}O_{10}]^{\bullet+}$ ($x=2,3$),[13c,37] $[Ce_xV_yO_z]^+$ ($x+y=2,\ 3;\ z=4,\ 5,\ 6$),[38] $[ZrScO_4]^{\bullet}$ and $[ZrNbO_4]^{\bullet}$.[39] Again, a high spin density located at a terminal oxygen atom is common for all these systems, and, furthermore, all cationic clusters except for the cerium-containing systems have been probed experimentally and found to be reactive in terms of thermal HAT from methane. In the context of site-selectivity, the studies of heteronuclear oxide systems permit the question of which M=O unit actually bears the radical oxygen atom to be addressed. For example, the radical site in $[VAlO_4]^{\bullet+}$ is predicted to correspond to a terminal Al–$O_t^{\bullet}$ group, no unpaired spin density is located at the vanadium-bound oxygen atom.[16] Further, and most importantly in the present context, it is the Al–$O_t^{\bullet}$ moiety which is involved in HAT from methane under thermal

conditions; according to DFT calculations, the V=O_t unit is completely inert in this respect.[16] Similar results have been computationally derived for various silicon- and phosphorous-containing cluster ions; the high spin density is mostly localized at the main-group atom-bound moiety, that is, Si–$O_t^{\bullet}$ and P–$O_t^{\bullet}$, which correspond to the reactive sites of the clusters (Figure 5).[13c,21,37] Clearly, an experimental verification of these interesting theoretical findings by, for example, gas-phase IR spectroscopy is highly desirable.[40]

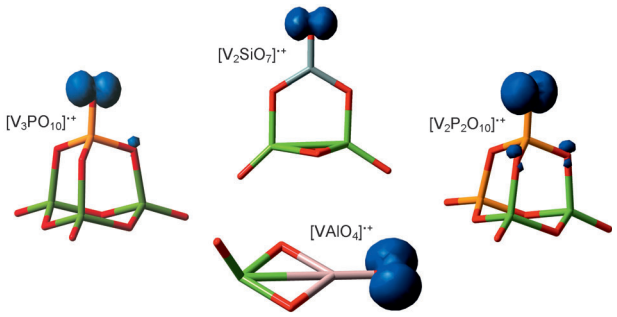

Figure 5. Lowest-energy structures calculated for $[VAlO_4]^{\bullet+}$, $[V_2SiO_7]^{\bullet+}$, $[V_3PO_{10}]^{\bullet+}$, and $[V_2P_2O_{10}]^{\bullet+}$ using DFT with the UB3LYP/TZVP level of theory (green V, gray Si, pink Al, yellow P, red O). The blue isosurface indicates the spin density as the reactive site of the respective cluster.

Detailed DFT calculations of the structurally related $[V_3PO_{10}]^{\bullet+}/[V_4O_{10}]^{\bullet+}$ systems in their HAT reactions with methane also indicate that a high spin density at the terminal oxygen atom of the reactive species does matter. As described above for the homonuclear vanadium oxide cluster $[V_4O_{10}]^{\bullet+}$, the hydrogen-atom abstraction from methane is also barrierless for $[V_3PO_{10}]^{\bullet+}$, provided CH_4 approaches the radical P–$O_t^{\bullet}$ unit of the cluster. With regard to the overall energetics of HAT, the reaction is also thermochemically possible at a V=O_t unit of either $[V_3PO_{10}]^{\bullet+}$ or $[V_4O_{10}]^{\bullet+}$ which have no spin density at the oxygen atom; however, the unpaired electron has to be transferred to the reactive site in the course of the reaction. Clearly, this intramolecular spin-density transfer is a prerequisite to "prepare" the active site and to accept the hydrogen, and this process requires a promotion energy. Thus, a barrier—albeit low for $[V_4O_{10}]^{\bullet+}$—is involved when HAT commences at a V=O_t unit, in contrast to the barrier-free reaction starting at the P–$O_t^{\bullet}$ and V–$O_t^{\bullet}$ units of $[V_3PO_{10}]^{\bullet+}$ or of $[V_4O_{10}]^{\bullet+}$, respectively; the P–$O_t^{\bullet}$ and V–$O_t^{\bullet}$ units are already in a state to engage in HAT.[37,41] With or without methane being involved, the barrier for an intramolecular spin-density transfer decreases in going from $[V_3PO_{10}]^{\bullet+}$ to $[V_4O_{10}]^{\bullet+}$ to $[P_4O_{10}]^{\bullet+}$ in line with the increasing HAT reactivity observed in the experiments (relative rate constants 1:2.5:2.9); although less pronounced, the same trend has been confirmed in a different experimental setup.[13c] Further, the concept of an intramolecular spin-density transfer can also be applied to other small, highly symmetric clusters and helps to explain HAT reactivity, as for example, for $[SO_2]^{\bullet+}$. In the ground state, the spin in $[SO_2]^{\bullet+}$ is almost equally distributed among the atoms, namely 30% on the sulfur and 35% on each of the two oxygen atoms. However, the approach of the hydrocarbon induces an intramolecular spin-density transfer to localize most of the spin at one of the terminal oxygen-atoms, which then brings about homolytic C–H bond scission of methane, concomitant with the final spin-transfer to the incipient $CH_3^{\bullet}$ radical. Such intrinsic spin-changes to form an active site for C–H bond abstraction have been also observed in the oxidation of methane by the biological relevant $[(Por)Fe^{IV}O]^{\bullet+}$ system.[42]

3.2. Open-Shell versus Closed-Shell Systems and the Role of the Spin State

Until recently, no *even*-electron oxo-species was known which brings about thermal HAT from methane in the gas phase. However, *even*-electron $[CuO]^+$,[11] which, a decade ago, had already been predicted to be a powerful candidate to mediate the methane-to-methanol conversion,[43] has lately been generated in the gas phase and observed to be capable of activating methane. The reaction gives rise to branching ratios of 40 to 60% for the homolytic C–H bond scission and $CH_4 \rightarrow CH_3OH$ conversion, respectively, with a two-state reactivity scenario being responsible for the chemoselectivities.[11] High-level quantum chemical calculations revealed that the high-spin, O_2-like state (triplet) corresponds to the ground state of $[CuO]^+$;[44] a similar bonding situation has also been reported for other late transition-metal oxides.[12a,26a,43,45] Thus, $[CuO]^+$ has a biradicaloid π bonding with two degenerate singly occupied π orbitals which correspond to the antibonding π* orbital of $[CuO]^+$. These orbitals have a relatively strong contribution from the $2p_\pi$ orbital of oxygen, thus resulting in a crucial high spin density of 1.68 at the oxygen atom and of only 0.32 at Cu (Figure 6). In other words, cationic copper oxide can be regarded as $[Cu^{II}–O^{\bullet}]^+$, rather than the formally higher oxidized Cu^{III} species $[Cu^{III}=O]^+$.

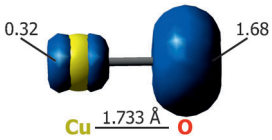

Figure 6. Triplet ground-state of $[CuO]^+$. The spin density is given in numbers and indicated by the blue isosurface.

As to the reaction of $[CuO]^+$ with methane, this process can be classified in terms of an indirect HAT pathway (Figure 7): After coordination of the carbon atom to the copper site of the ground-state cation, the reactions proceeds via ^{3}**TS1–2**, delivering the hydrocarbon atom to the oxygen where C–H bond activation occurs, thus resulting in the formation of an O–H bond, and repositioning of the methyl ligand to give the linear arrangement in ^{3}**2**. Next, the methyl group can either be liberated to give the spin-allowed HAT product, or in a rebound-step is transferred to the oxygen atom, leading to the formation of $^3[Cu(CH_3OH)]^+$ (^{3}**3**); however, formation of free CH_3OH in a spin-allowed process $^3\mathbf{3} \rightarrow {}^3[Cu]^+ + CH_3OH$ is endothermic by 29 kJ mol^{-1}. Instead, formation of CH_3OH requires an intersystem crossing (ISC)

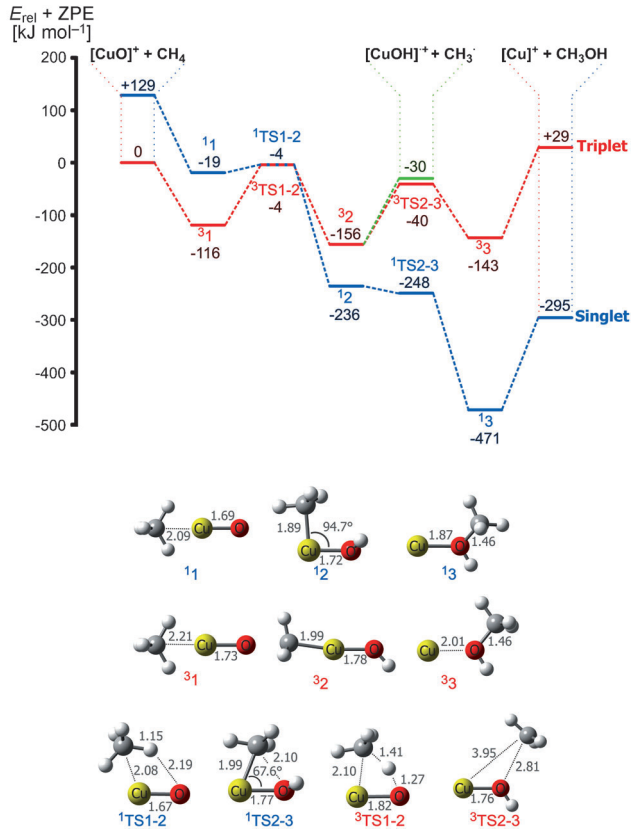

Figure 7. Potential-energy surface for the reaction of $[CuO]^+$ with CH_4 (blue = singlet, red = triplet) and the associated structures of the intermediates and transition structures, calculated at the CBS-QB3 level of theory. Relative energies, corrected for zero-point energy contributions are given in kJ mol^{-1} and relevant bond lengths in Å (adapted from Ref. [11]).

to the singlet surface, a pathway that is extremely exothermic (-295 kJ mol^{-1}). Since the two geometrically quite different transition structures ^{1,3}**TS1–2** are almost isoenergetic, the ISC to the singlet-surface occurs either closely before or directly after passing through **TS1–2**. Interestingly, the rate-determining step for both pathways corresponds to the initial cleavage of the inert C–H bond of methane for which the spin density at the abstracting atom is crucial, while for the oxygen-atom transfer to form methanol in a rebound-step, a spin-flip to the singlet state is essential in the course of the reaction. Another diatomic system is worth mentioning in this context, that is, calcium oxide CaO: A computational study on the *closed-shell* CaO/CH_4 system suggests that while H-atom abstraction is slightly exothermic, the reaction is impeded by a significant barrier.[46] On the other hand, removal of one electron leads to the *open-shell* $[CaO]^{\bullet+}/CH_4$ system in which the spin is mainly localized at the oxygen atom; not surprisingly, HAT in the thermal reaction with methane has been observed.[28]

In addition to these small diatomic systems, similar observations have been made for larger clusters. For example, main-group aluminum-oxide clusters are capable of bringing about efficient C–H bond scission of methane at room temperature.[14] However, only those clusters having an *even* number of aluminum atoms $[(Al_2O_3)_x]^{\bullet+}$ ($x = 3$–5) are reactive, for example, $[Al_8O_{12}]^{\bullet+}$, Equation (1), while clusters with an *odd* number of aluminum atoms do not react with CH_4, for example, $[Al_7O_{11}]^+$, Equation (2).

$$[Al_8O_{12}]^{\bullet+} + CH_4 \rightarrow [Al_8O_{11}(OH)]^+ + CH_3^{\bullet} \quad (1)$$

$$[Al_7O_{11}]^+ + CH_4 \not\rightarrow [Al_7O_{10}(OH)]^{\bullet+} + CH_3^{\bullet} \quad (2)$$

One of the crucial differences between these two systems concerns the distribution of the spin within the clusters. While in the doublet ground-state of $[Al_8O_{12}]^{\bullet+}$ the spin is exclusively localized at one terminal oxygen atom, thus representing an oxygen-centered radical, in the triplet ground-state of $[Al_7O_{11}]^+$ the spin is distributed among four oxygen atoms, each one carrying approximately 0.5 (Figure 8). Thus, this cluster is lacking an unpaired electron localized at one oxygen atom, and its lack of reactivity underlines once more the importance of oxygen-centered radicals to bring about thermal hydrogen-atom abstraction from methane.[14]

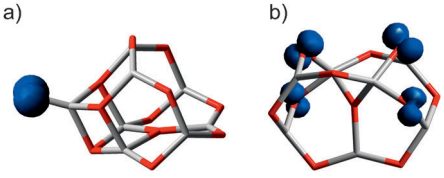

Figure 8. Lowest-lying doublet ground-state of $[Al_8O_{12}]^{\bullet+}$ (a) and triplet ground-state of $[Al_7O_{11}]^+$ (b), derived from DFT/UB3LYP calculations (gray Al, red O). The spin density is indicated by the blue isosurface.

With regard to the reaction mechanism, the reaction of $[Al_8O_{12}]^{\bullet+}$ with CH_4 (Figure 9a) follows a direct HAT pathway. Methane coordinates to the cluster **4** through the terminal oxygen atom and the reaction proceeds, via the encounter complex **5** and the transition structure **TS5–6**, in a quasi barrier-free process to the intermediate **6** from which finally the ionic cluster product **7** and a methyl radical are generated. In contrast, in the reaction of $[Al_7O_{11}]^+$ **8** with CH_4 (Figure 9b), in the first step a significantly more stable adduct complex **9** is generated by coordination of the substrate to the vacant site of an aluminum atom. Next, from **9**, HAT can only proceed via the energetically demanding transition state **TS9–10** to form **10**.

A further comparison of these two PESs is quite revealing: First, both reactions are exothermic and therefore thermochemically allowed. Not entirely unexpected, HAT to the terminal oxygen atom of $[Al_8O_{12}]^{\bullet+}$ is energetically favored by approximately 45 kJ mol^{-1} over the couple $[Al_7O_{11}]^+/CH_4$; nevertheless, HAT to a bridging oxygen atom in $[Al_7O_{11}]^+$ is also energetically feasible and significantly exothermic. Second, and more importantly, although both HAT processes are exothermic, the kinetic barriers differ strongly. In the doublet $[Al_8O_{12}]^{\bullet+}/CH_4$ system, the initial interaction between the oxygen-centered radical in the cluster and the C–H bond of methane enables a barrier-free C–H bond scission; in contrast, HAT to an oxygen atom of $[Al_7O_{11}]^+$ is not favored kinetically. Thus, the heights of the two intrinsic barriers **TS5–6** and **TS9–10** for HAT starting

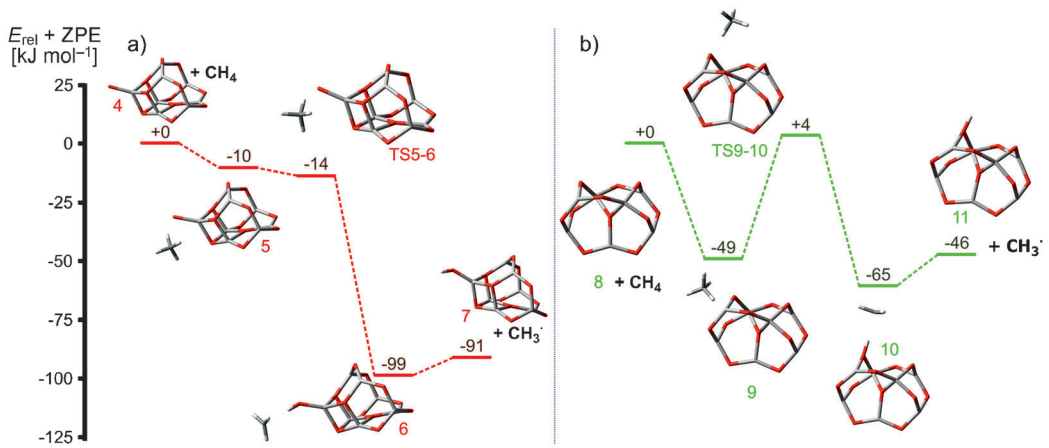

Figure 9. Potential-energy surfaces for the reactions of $[Al_8O_{12}]^{\bullet+}$ (a) and $[Al_7O_{11}]^+$ (b) with CH_4 and the associated structures of the intermediates and transition structures, at the UB3LYP/TZVP level of theory. Relative energies, corrected for zero-point energy contributions, are given in kJ mol^{-1}.

from the intermediates **5** and **9**, respectively, are negligible for the $[Al_8O_{12}]^+/CH_4$ system but substantial for the $[Al_7O_{11}]^+/CH_4$ couple. The significantly lower spin density at a particular oxygen atom of the $[Al_7O_{11}]^+$ oxide, as well as the fact that the reactive site is a bridging oxygen atom, increase the activation barrier for the C–H bond cleavage such that the respective transition state **TS9–10** is higher in energy than the entrance channel and therefore not accessible in a thermal ion/molecule reaction, as observed experimentally in the gas phase.[47]

Similar observations have been made for the reactivity of the $[(MgO)_x]^{\bullet+}$ ($x = 1$–7) clusters towards methane and other small hydrocarbons; while $[MgO]^{\bullet+}$ brings about HAT from CH_4, the larger clusters are completely inert towards methane, even though the reactions are exothermic.[23] For example, in $[(MgO)_2]^{\bullet+}$ the spin is equally distributed over the two oxygen atoms of the cluster; intracluster spin-density transfer and the associated kinetic barrier for the C–H bond activation of methane are too high in energy to be accessible under thermal conditions, resulting in a barrier of 20 kJ mol^{-1} above the entrance channel. Further, the $[(MgO)_7]^{\bullet+}$ cluster is the only species among the magnesium oxide cations investigated in which the radical is located at only one of the bridging oxygen atoms; compared to the other magnesium oxide clusters, $[(MgO)_7]^{\bullet+}$ has to overcome the lowest computed barrier in the reaction with methane which is reduced to -0.5 kJ mol^{-1} including the zero-point energy correction.[48] Thus, although bridging oxygen atoms are not as reactive as terminal oxygen atoms, the presence of spin density also counts in these systems. For example, HAT reactions mediated by $[(MgO)_2]^{\bullet+}$ are only observed with those substrates that have C–H bonds which are much weaker than the one of methane, for example, propane or butane,[23] while the silver oxide cluster $[Ag_2O]^{\bullet+}$, carrying a truly oxygen-centered radical at the bridging oxygen atom, enables the efficient activation of ethane under ambient conditions.[49] Additional spectroscopic and reactivity studies on larger $[(MgO)_x]^{\bullet+}$ clusters ($x = 2$–7) support these findings.[50]

The presence of an oxygen-centered radical in other transition-metal oxide (TMO) clusters has also been suggested to be responsible for their reactivity towards methane.[41,51] Based on experimental and theoretical studies on various larger TMO clusters, it was found that clusters of $M_xO_y^q$ stoichiometry contain oxygen-centered radicals if they satisfy the general Equation (3), in which n is the number of valence electrons of the metal M.

$$\Delta \equiv 2y - nx + q = 1 \qquad (3)$$

According to B3LYP calculations, the prediction of an oxygen-centered radical holds true for a large number of early transition-metal oxides clusters $M_xO_y^q$ (M = Groups 3–7; $x = 1$–3; and, according to Equation (3), y is defined by the criteria $\Delta = 1$; Figure 10a);[52] several series of these stoichiometric early transition-metal oxide clusters fulfilling the $\Delta = 1$ criteria were successfully probed with respect to their HAT reactivity towards methane, including $[(TiO_2)_{1-5}]^{\bullet+}$,

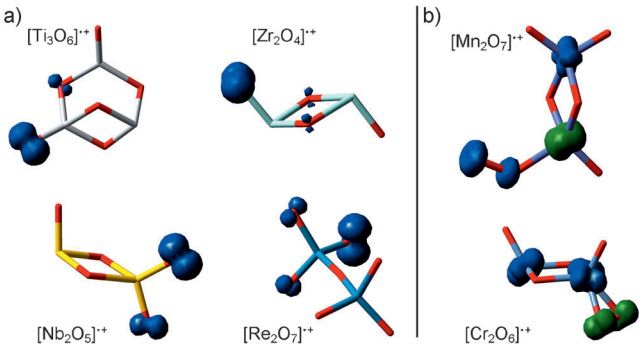

Figure 10. Lowest-energy structures calculated for selected early transition-metal oxide clusters with $\Delta = 1$ [see Eq. (3)]; white Ti, cyan Zr, violet Mn, yellow Nb, turquoise Re, silver Cr, red O). The blue isosurfaces indicate the spin density (green indicates opposite sign). Clusters with an oxygen-centered radical (a) are reactive towards methane, whereas those with an intact O–O bond lacking an oxygen-centered radical (b) do not bring about HAT from methane under thermal conditions.

$[(ZrO_2)_{1-4}]^{\bullet+}$, $[(HfO_2)_{1-2}]^{\bullet+}$, $[(MoO_3)_{1-2}]^{\bullet+}$, $[(WO_3)_{1-3}]^{\bullet+}$, $[(V_2O_5)_{1-5}]^{\bullet+}$, $[(Nb_2O_5)_{1-3}]^{\bullet+}$, $[(Ta_2O_5)_{1-2}]^{\bullet+}$, and $[Re_2O_7]^{\bullet+}$.[17,18,53] In contrast, the oxide clusters with $\Delta \neq 1$ were completely inert in their thermal reactions with methane. However, a few exceptions are known which, while satisfying Equation (3), do not have oxygen-centered radicals, these are, oxide clusters of chromium and manganese: $[(CrO_3)_{1-3}]^{\bullet+}$, $[(CrO_3)_{2-3}O]^{\bullet-}$, $[MnO_4]^{\bullet}$, $[Mn_2O_7]^{\bullet+}$, $[Mn_2O_8]^{\bullet-}$, and $[Mn_3O_{11}]^{\bullet}$. As revealed by DFT calculations, these clusters have a different bonding pattern; in fact, super-oxide or molecular oxygen units with intact O–O bonds are present in these clusters instead of terminal bound oxides as found for the early TMOs (Figure 10b). These structural features of Cr and Mn oxides are in line with the smallest bond energies among the transition-metal oxides of Groups 3–7 (CrO 462.2 kJ mol^{-1}) and MnO 369.5 kJ mol^{-1})[54] as well as the larger bond energy of O_2 (494.0 kJ mol^{-1}).[55] Accordingly, cationic $[(CrO_3)_{1-2}]^{\bullet+}$ and $[Mn_2O_7]^{\bullet+}$ do not react with methane. More surprisingly, the distinctive reactivity pattern of oxides of manganese and chromium in the gas phase, compared to those of the other early transition metals, also prevails with respect to HAT in the condensed phase; among the rare examples for liquid-phase HAT involving weaker C–H bonds by *closed shell* oxo-systems, the most cited systems are the oxides of these very elements, that is, $[MnO_4]^-$ and CrO_2Cl_2.[29b,56] Clearly, the oxides of manganese and chromium exhibit particular, electronic features, and more accurate theoretical and experimental studies are necessary to uncover the reasons for this apparently deviating HAT reactivity.

3.3. Cationic versus Anionic and Neutral Systems

Gas-phase experiments based on mass spectrometry generally employ charged species, and experimental investigations of *neutral* clusters are rather scarce owing to the difficulties in the experimental setups; consequently, only a few studies, mainly on vanadium oxides, are known.[39,57] Computations predict, for example, for $V_3O_8^{\bullet}$ or $VO_3^{\bullet}$, a V–O$^{\bullet}$ moiety as the reactive site; however, most experiments are conducted with unsaturated hydrocarbons, such as ethylene or acetylene, in which oxygen-atom transfer and C=C bond cleavage prevail. In general, neutral species are considered as less reactive than cationic metal oxides. In the reaction with C_2H_4, however, calculations predict a higher reactivity of neutral $VO_3^{\bullet}$ compared to cationic VO_3^+ which has a peroxo unit and no spin density at an oxygen atom.[57a] The reactivity of neutral vanadium oxide clusters towards ethane has also been investigated; however, adduct formation was the only observed reaction channel.[57a]

Also the reactivity of negatively charged transition-metal oxide clusters was found to be significantly lower than that of the cationic analogues.[34,35,58] However, spin density does also count for these systems. Despite the observation that metal oxide cluster anions are generally less reactive towards saturated hydrocarbons, HAT from ethane[34] and *n*-butane[35,58d,59] mediated by anionic oxide clusters has been observed in recent studies, and each of the systems possesses an oxygen-centered radical. In a comparative study of cationic $[V_2O_5]^{\bullet+}$, neutral $[V_3O_8]^{\bullet}$, and anionic $[V_2O_6]^{\bullet-}$ oxo clusters,[41,58b] it was demonstrated that the anionic $[V_2O_6]^{\bullet-}$ exhibits the lowest reactivity towards methane; however, the activation barrier of 25.1 kJ mol^{-1} (Figure 11a) is still significantly lower compared to other related metal oxide clusters

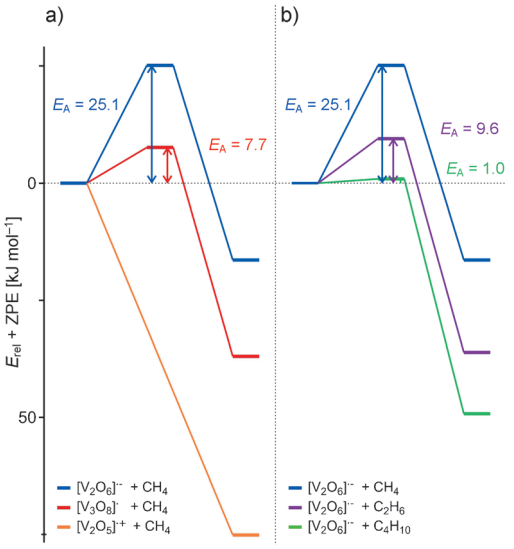

Figure 11. Schematic potential-energy surfaces for the HAT a) of selected vanadium oxide clusters from methane and b) of the anionic cluster $[V_2O_6]^{\bullet-}$ from methane, ethane, and *n*-butane. The relative energies for the activation energies (E_As), products and educts are corrected for zero-point energy and given in kJ mol^{-1} (adapted from Ref. [41]).

lacking an oxygen-centered radical, for example, $V_3O_6Cl_3$, Cr_3O_9, or Mo_3O_9 (164–367 kJ mol^{-1}).[60] As expected, the barrier decreases when going to larger hydrocarbons (Figure 11b), and becomes small enough for $[V_2O_6]^{\bullet-}$ or $[Zr_2O_5]^{\bullet-}$, for example, to bring about homolytic C–H bond activation of *n*-C_4H_{10} at rather mild conditions.[41,58b,c] Further, the rate constant $k([Zr_2O_5]^{\bullet-} + CH_4)$ has been estimated to approximately 6.6×10^{-15} cm^3 s^{-1} molecule^{-1},[41] which is close to the rate constant reported for the reaction of hydroxyl radicals with methane, $k([OH]^{\bullet} + CH_4) = 7.89 \times 10^{-15}$ cm^3 s^{-1} molecule^{-1}.[61] Thus, the anionic oxide cluster $[Zr_2O_5]^{\bullet-}$ having an oxygen-centered radical is as reactive as the free hydroxyl radical in terms of the homolytic C–H bond fission and HAT from hydrocarbons.

4. HAT in Heterogeneous Catalysis at Room Temperature: Spin Does Count!

Gas-phase clusters have been proposed to serve as models for heterogeneous catalysis.[12e,40,62] Thus, if these studies are of any relevance for real catalytic systems, oxygen-centered radicals should also play an important role in the chemistry at complex surfaces. One well-known example concerns the Lunsford mechanism for the oxidative coupling of methane (OCM) on lithium-doped magnesium oxides (Figure 12).[63] OCM involves both a heterogeneous component on metal oxide surfaces, and a homogeneous part in the gas phase in

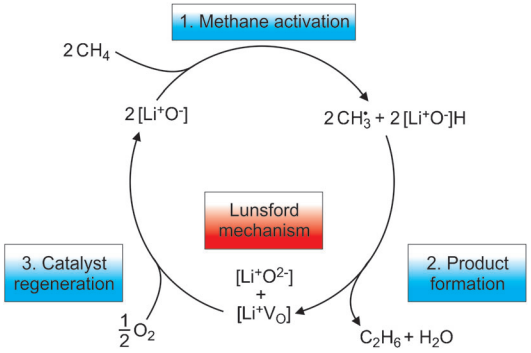

Figure 12. The postulated Lunsford mechanism for the oxidative coupling of methane (adapted from Ref. [64b]).

which the coupling of the free methyl radicals occurs followed by dehydrogenation of C_2H_6 to form C_2H_4. Much of the current debate[64] focus on the nature of the active site of metal oxide surfaces, which, according to Lunsford's suggestion,[63a,65] corresponds to an oxygen-centered radical. Several hypotheses about the possible formation of these radical sites exist; for example, in the context of oxidation processes mediated by molybdenum oxide catalysts, it was assumed that, at sufficiently high temperatures, the radical site may be formed by an electron transfer from the oxygen ligand to the metal cation (Figure 13).[66] Owing to their rather low thermal stability and the difficulties in investigating the complex processes on real surfaces at elevated temperatures, an experimental confirmation of the existence of these reactive sites is still missing. In contrast, no controversy exists as to the rate-limiting step of OCM, and the consensus view assigns this

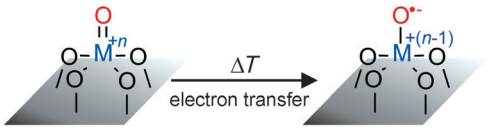

Figure 13. Postulated electron transfer from the oxygen ligand to the metal cation to form M–O•⁻ as the reactive site in high-temperature catalysis.

to the hydrogen-atom transfer from methane to an oxygen atom on the surface.[67] Interestingly, more recent surface studies[68] demonstrate that this C–H bond cleavage can be achieved by systematically generated radical M–O• moieties, also often referred to as M–O⁻ or M–O•⁻, at ambient conditions; these examples will be presented below.

In addition to the oxidative coupling to C_2H_x ($x = 4, 6$), the selective oxidation of methane to C_1 oxygenates also depends on the very first step, that is, C–H bond activation. With respect to the methane-to-methanol conversion, zeolites ZSM-5 proved to be a valuable reagent when doped with metal oxides.[68] Typically, the reactive metal oxide sites are generated in situ by first doping with bare metal atoms and subsequent oxidation with N_2O or pure oxygen;[68b,c,69] especially iron and copper showed remarkable selectivities in the oxidation of methane.[68b–d] In analogy, this process is performed in nature by the metalloenzymes methane monooxygenases (MMOs);[70] soluble MMO (sMMO) contains a well-characterized doubly oxygen-bridged di-iron cluster while the reactivity of particulate MMO (pMMO), after a long controversy about the nature of its active site, has been shown to depend on copper.[71] As revealed by carefully conducted studies on iron-doped zeolites Fe-ZSM-5, so called α-sites are formed at high temperatures.[72] These α-sites correspond to Fe^{II} moieties which are produced from auto-reduction of Fe^{III} to Fe^{II} concomitant with the evolution of O_2. Further, the $(Fe^{II})_\alpha$ sites can be oxidized by use of N_2O, generating the highly active radical oxygen species $(Fe^{III}–O^{\bullet-})_\alpha$;[73] the existence of this complex has been confirmed by applying numerous techniques, including Mössbauer or electron-paramagnetic resonance spectroscopy.[74] Fe-ZSM-5 exhibits a remarkable reactivity towards methane at room temperature: It selectively activates methane to methanol as the only observed reaction product.[68b,d] As found in mechanistic studies with CH_2D_2, the KIE amounts to 1.9 to 5.5 (+100° to −50 °C), thus indicating that the rate-limiting step corresponds to the cleavage of the C–H bond. Furthermore, based on the exclusive formation of methanol, it was assumed that the reaction pathway occurs as a single-step process leading directly to adsorbed methanol on the surface (Figure 14a).[75]

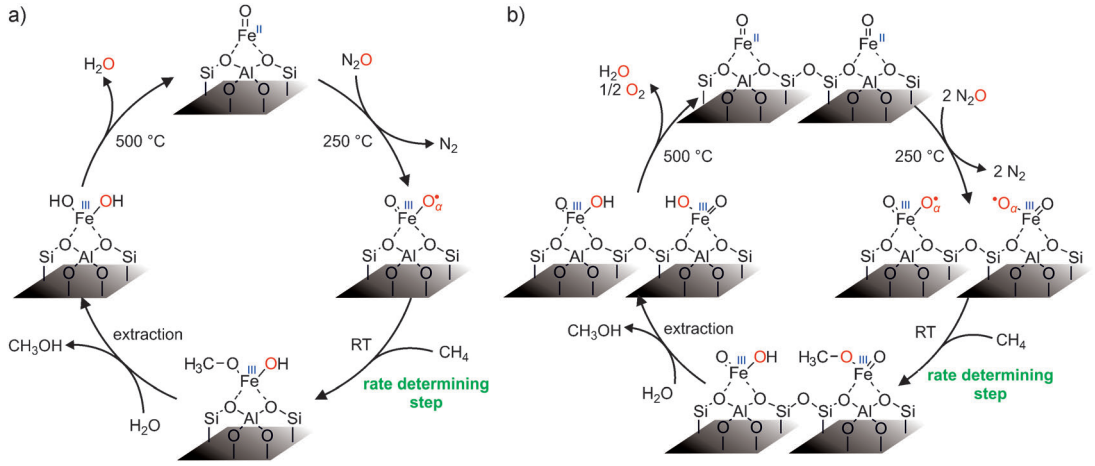

Figure 14. Catalytic cycles for the oxidation of CH_4 by N_2O over Fe-ZSM-5. Mechanistic studies suggest that the reaction proceeds as a combination of both pathways, either at a single (a) or at two adjacent $(Fe^{III}–O^{\bullet-})_\alpha$ sites (b). Cycle (a) is identical to that described by Wood et al.[78] See text for details.

However, the ratio of CH_4 to the number of α-oxygen sites is 1:1.8, thus suggesting more than one $(Fe^{III}–O^{\bullet-})_\alpha$ site is involved in the reaction.[76] As revealed by IR spectroscopy, HAT from methane to one $(Fe^{III}–O^{\bullet-})_\alpha$ site leads to a newly formed hydroxy group and the resulting methyl radical recombines with another α-site forming a surface-bound methoxy group (Figure 14b);[68b,77] hydrolysis of the methoxy groups then results in the formation of methanol.[78] The deviation from the expected 1:2 ratio can be explained by a combination of the two different reaction pathways (Figure 14);[68d] for both of them, however, the initial C–H bond activation step is rate determining.

Another recent example for homolytic C–H bond activation of methane at room temperature on surfaces is given by pure silica zeolites which can be activated by deep UV photolysis with wavelengths about 165 or 180 nm.[79] The radiation induces homolytic cleavage of the O–H bonds of the silanol groups on the surface, thus generating a hydrogen atom and a surface-bound silyloxyl radical, which then brings about HAT from methane. The so formed methyl radicals subsequently combine either to form hydrocarbons or, in the presence of molecular oxygen, to oxygenated species; the selective oxidation of methane to methanol in the presence of O_2 is due to the confined space of the zeolite pores in which the reactions take place thus restricting the mobility of the radical intermediates.[79] To conclude, these examples from heterogeneous catalysis may indicate that the systematic generation of radicals on the surface triggers homolytic C–H bond activation of methane at room temperature.

5. Conclusion

The examples highlighted herein provide compelling arguments for the importance of oxygen-centered radicals in gas-phase (ion) chemistry with respect to the homolytic C–H bond cleavage of methane and other inert substrates: All the reactive species capable of an efficient hydrogen-atom abstraction from methane at room temperature have a terminal oxygen-centered radical; on the other hand, if the radical is delocalized over a few centers, or when the abstracting atom has no unpaired spin density, significantly higher activation barriers exist. The concept of intramolecular spin-density transfer indicates that HAT reactions by non-radical reactive sites might be possible but in such cases energy is necessary to fulfill the electronic and structural requirements for homolytic C–H bond scission. These two steps (establishing the correct electronic and geometric structures and performing the actual HAT) can be concurrent or they can occur sequentially depending on the actual system. Cleary, it costs an energetic price to form a "prepared" state, and this "preparation energy" can be part of the activation energy which does not correlate with the free energy of reaction.[80] The role of spin density located at the reactive site of a catalyst is also emphasized by recent surface studies on the methane-to-methanol conversion; the directed formation of oxygen-centered radicals on the surface of zeolites enables the initial activation of the C–H bond of methane at room temperature. These examples may provide important mechanistic insights for other catalytic oxidation processes, emphasizing the idea of radical formation on the oxide-surface to bring about, for example, oxidative coupling or the conversion of methane into methanol. In short: The general statement in Ref. [1] about the unimportance of unpaired spin density at the hydrogen-abstracting atom finds no support in the combined experimental/computational work described herein; rather, the statement is quite misleading.[81]

This research was sponsored by the Fonds der Chemischen Industrie and the Deutsche Forschungsgemeinschaft (DFG), in particular the Cluster of Excellence "Unifying Concepts in Catalysis" (coordinated by the Technische Universität Berlin and funded by the DFG). We particularly appreciate insightful discussions with Prof. James M. Mayer, Prof. Joachim Sauer, and Prof. Sason Shaik, helpful comments by the reviewers, as well as valuable practical and conceptual contributions of past and present co-workers.

Received: November 28, 2011
Published online: March 16, 2012

[1] J. M. Mayer, *Acc. Chem. Res.* **2011**, *44*, 36.
[2] a) J. T. Hynes, J. P. Klinman, H.-H. Limbach, R. L. Schowen, *Hydrogen-Transfer Reactions*, Wiley-VCH, Weinheim, New York, **2006**; b) M. H. V. Huynh, T. J. Meyer, *Chem. Rev.* **2007**, *107*, 5004; c) J. J. Warren, T. A. Tronic, J. M. Mayer, *Chem. Rev.* **2010**, *110*, 6961.
[3] a) C. Limberg, *Angew. Chem.* **2003**, *115*, 6112; *Angew. Chem. Int. Ed.* **2003**, *42*, 5932; b) J. Sauer in *Computational Modeling for Homogeneous and Enzymatic Catalysis* (Ed.: K. Morokuma, J. Musaev), Wiley-VCH, Weinheim, **2008**, p. 231; c) L. Que, W. B. Tolman, *Nature* **2008**, *455*, 333; d) C. Limberg, *Angew. Chem.* **2009**, *121*, 2305; *Angew. Chem. Int. Ed.* **2009**, *48*, 2270; e) S. Shaik, H. Chen, D. Janardanan, *Nat. Chem.* **2011**, *3*, 19.
[4] a) O. Tishchenko, D. G. Truhlar, A. Ceulemans, M. T. Nguyen, *J. Am. Chem. Soc.* **2008**, *130*, 7000; b) S. Hammes-Schiffer, A. V. Soudackov, *J. Phys. Chem. B* **2008**, *112*, 14108; c) A. Sirjoosingh, S. Hammes-Schiffer, *J. Phys. Chem. A* **2011**, *115*, 2367.
[5] M. G. Evans, M. Polanyi, *Trans. Faraday Soc.* **1938**, *34*, 11.
[6] a) A reviewer has pointed out, that Mayer's analyses "are by nature log–log plots where anything not too wild will look linear over a small enough range. The fact that experimental points fall on a single line in a linear-free-energy relationship is NOT evidence that everything proceeds by the same mechanism … thus, Mayer's linear correlations probably do not exclude, for example, that all PCET are really HAT reactions or vice versa or something in between." b) Also, see: A. Butler, *Chem. Br.* **1989**, *25*, 997.
[7] a) J. M. Mayer, *Annu. Rev. Phys. Chem.* **2004**, *55*, 363; b) J. M. Mayer, *J. Phys. Chem. Lett.* **2011**, *2*, 1481.
[8] R. A. Marcus, *Angew. Chem.* **1993**, *105*, 1161; *Angew. Chem. Int. Ed. Engl.* **1993**, *32*, 1111.
[9] S. Shaik, A. Shurki, *Angew. Chem.* **1999**, *111*, 616; *Angew. Chem. Int. Ed.* **1999**, *38*, 586.
[10] a) A. M. Khenkin, D. Kumar, S. Shaik, R. Neumann, *J. Am. Chem. Soc.* **2006**, *128*, 15451; b) D. Balcells, C. Raynaud, R. H. Crabtree, O. Eisenstein, *Inorg. Chem.* **2008**, *47*, 10090.
[11] N. Dietl, C. van der Linde, M. Schlangen, M. K. Beyer, H. Schwarz, *Angew. Chem.* **2011**, *123*, 5068; *Angew. Chem. Int. Ed.* **2011**, *50*, 4966.
[12] a) D. Schröder, H. Schwarz, *Angew. Chem.* **1995**, *107*, 2126; *Angew. Chem. Int. Ed. Engl.* **1995**, *34*, 1973; b) D. Schröder, H.

Schwarz, *Proc. Natl. Acad. Sci. USA* **2008**, *105*, 18114; c) G. E. Johnson, E. C. Tyo, A. W. Castleman, *Proc. Natl. Acad. Sci. USA* **2008**, *105*, 18108; d) M. Schlangen, H. Schwarz, *Dalton Trans.* **2009**, 10155; e) G. E. Johnson, R. Mitric, V. Bonacic-Koutecký, A. W. Castleman, Jr., *Chem. Phys. Lett.* **2009**, *475*, 1; f) J. Roithová, D. Schröder, *Chem. Rev.* **2010**, *110*, 1170; g) H. Schwarz, *Angew. Chem. Int. Ed.* **2011**, *50*, 10096; h) X.-L. Ding, X.-N. Wu, Y.-X. Zhao, S.-G. He, *Acc. Chem. Res.* **2011**, DOI: 10.1021/ar2001364.

[13] a) S. Feyel, J. Döbler, D. Schröder, J. Sauer, H. Schwarz, *Angew. Chem.* **2006**, *118*, 4797; *Angew. Chem. Int. Ed.* **2006**, *45*, 4681; b) N. Dietl, M. Engeser, H. Schwarz, *Angew. Chem.* **2009**, *121*, 4955; *Angew. Chem. Int. Ed.* **2009**, *48*, 4861; c) N. Dietl, R. F. Höckendorf, M. Schlangen, M. Lerch, M. K. Beyer, H. Schwarz, *Angew. Chem.* **2011**, *123*, 1466; *Angew. Chem. Int. Ed.* **2011**, *50*, 1430.

[14] S. Feyel, J. Döbler, R. Höckendorf, M. K. Beyer, J. Sauer, H. Schwarz, *Angew. Chem.* **2008**, *120*, 1972; *Angew. Chem. Int. Ed.* **2008**, *47*, 1946.

[15] D. Schröder, A. Fiedler, J. Hrušák, H. Schwarz, *J. Am. Chem. Soc.* **1992**, *114*, 1215.

[16] Z. C. Wang, X. N. Wu, Y. X. Zhao, J. B. Ma, X. L. Ding, S. G. He, *Chem. Phys. Lett.* **2010**, *489*, 25.

[17] J. N. Harvey, M. Diefenbach, D. Schröder, H. Schwarz, *Int. J. Mass Spectrom.* **1999**, *182*, 85.

[18] I. Kretzschmar, A. Fiedler, J. N. Harvey, D. Schröder, H. Schwarz, *J. Phys. Chem. A* **1997**, *101*, 6252.

[19] G. de Petris, A. Troiani, M. Rosi, G. Angelini, O. Ursini, *Chem. Eur. J.* **2009**, *15*, 4248.

[20] X. N. Wu, Y. X. Zhao, W. Xue, Z. C. Wang, S. G. He, X. L. Ding, *Phys. Chem. Chem. Phys.* **2010**, *12*, 3984.

[21] X. L. Ding, Y. X. Zhao, X. N. Wu, Z. C. Wang, J. B. Ma, S. G. He, *Chem. Eur. J.* **2010**, *16*, 11463.

[22] M. F. Ryan, A. Fiedler, D. Schröder, H. Schwarz, *J. Am. Chem. Soc.* **1995**, *117*, 2033.

[23] D. Schröder, J. Roithová, *Angew. Chem.* **2006**, *118*, 5835; *Angew. Chem. Int. Ed.* **2006**, *45*, 5705.

[24] X. Zhang, H. Schwarz, *ChemCatChem* **2010**, *2*, 1391.

[25] K. Chen, Z.-C. Wang, M. Schlangen, Y.-D. Wu, X. Zhang, H. Schwarz, *Chem. Eur. J.* **2011**, *17*, 9619.

[26] a) S. Shaik, D. Danovich, A. Fiedler, D. Schröder, H. Schwarz, *Helv. Chim. Acta* **1995**, *78*, 1393; b) D. Schröder, S. Shaik, H. Schwarz, *Acc. Chem. Res.* **2000**, *33*, 139; c) S. Shaik, S. P. de Visser, F. Ogliaro, H. Schwarz, D. Schröder, *Curr. Opin. Chem. Biol.* **2002**, *6*, 556; d) J. N. Harvey, R. Poli, K. M. Smith, *Coord. Chem. Rev.* **2003**, *238–239*, 347; e) H. Schwarz, *Int. J. Mass Spectrom.* **2004**, *237*, 75; f) S. Shaik, H. Hirao, D. Kumar, *Acc. Chem. Res.* **2007**, *40*, 532.

[27] D. Schröder, J. Roithová, E. Alikhani, K. Kwapien, J. Sauer, *Chem. Eur. J.* **2010**, *16*, 4110.

[28] A. Božović, D. K. Bohme, *Phys. Chem. Chem. Phys.* **2009**, *11*, 5940.

[29] a) R. P. Bell, *Proc. R. Soc. London Ser. A* **1938**, *154*, 414; b) J. M. Mayer, *Acc. Chem. Res.* **1998**, *31*, 441.

[30] *Appl. Catal. A* **1997**, *157*, (the entire volume is dedicated to this topic).

[31] a) G. J. Hutchings, *J. Mater. Chem.* **2004**, *14*, 3385; b) J.-M. Millet, *Top. Catal.* **2006**, *38*, 83; c) Y. Taufiq-Yap, C. Goh, G. Hutchings, N. Dummer, J. Bartley, *Catal. Lett.* **2009**, *130*, 327; d) K. Kourtakis, L. Wang, E. Thompson, P. L. Gai, *Appl. Catal. A* **2010**, *376*, 40.

[32] N. Dietl, M. Engeser, H. Schwarz, *Chem. Eur. J.* **2010**, *16*, 4452.

[33] D. R. Justes, R. Mitric, N. A. Moore, V. Bonačic-Koutecký, A. W. Castleman, *J. Am. Chem. Soc.* **2003**, *125*, 6289.

[34] Z. C. Wang, X. N. Wu, Y. X. Zhao, J. B. Ma, X. L. Ding, S. G. He, *Chem. Eur. J.* **2011**, *17*, 3449.

[35] Y. X. Zhao, X. N. Wu, J. B. Ma, S. G. He, X. L. Ding, *J. Phys. Chem. C* **2010**, *114*, 12271.

[36] Z.-Y. Li, Y.-X. Zhao, X.-N. Wu, X.-L. Ding, S.-G. He, *Chem. Eur. J.* **2011**, *17*, 11728.

[37] J. B. Ma, X. N. Wu, X. X. Zhao, X. L. Ding, S. G. He, *Phys. Chem. Chem. Phys.* **2010**, *12*, 12223.

[38] L. Jiang, T. Wende, P. Claes, S. Bhattacharyya, M. Sierka, G. Meijer, P. Lievens, J. Sauer, K. R. Asmis, *J. Phys. Chem. A* **2011**, *115*, 11187.

[39] M. Nößler, R. Mitrić, V. Bonačić-Koutecký, G. E. Johnson, E. C. Tyo, A. W. Castleman, *Angew. Chem.* **2010**, *122*, 417; *Angew. Chem. Int. Ed.* **2010**, *49*, 407.

[40] K. R. Asmis, J. Sauer, *Mass Spectrom. Rev.* **2007**, *26*, 542.

[41] Y. X. Zhao, X. N. Wu, J. B. Ma, S. G. He, X. L. Ding, *Phys. Chem. Chem. Phys.* **2011**, *13*, 1925.

[42] S. Shaik, W. Lai, H. Chen, Y. Wang, *Acc. Chem. Res.* **2010**, *43*, 1154.

[43] Y. Shiota, K. Yoshizawa, *J. Am. Chem. Soc.* **2000**, *122*, 12317.

[44] E. Rezabal, J. Gauss, J. M. Matxain, R. Berger, M. Diefenbach, M. C. Holthausen, *J. Chem. Phys.* **2011**, *134*, 064304.

[45] D. Schröder, H. Schwarz, S. Shaik in *Metal-Oxo and Metal-Peroxo Species in Catalytic Oxidations*, Springer, Berlin, **2000**, S. 91.

[46] H.-Q. Yang, C.-W. Hu, S. Qin, *Chem. Phys.* **2006**, *330*, 343.

[47] In thermal ion/molecule reactions in the gas phase, the only available energy comes from the initial adduct formation. Therefore, intermediates or transition states above the entrance channel are not accessible.

[48] K. Kwapien, M. Sierka, J. Döbler, J. Sauer, *ChemCatChem* **2010**, *2*, 819.

[49] J. Roithová, D. Schröder, *J. Am. Chem. Soc.* **2007**, *129*, 15311.

[50] K. Kwapien, M. Sierka, J. Dobler, J. Sauer, M. Haertelt, A. Fielicke, G. Meijer, *Angew. Chem.* **2011**, *123*, 1754; *Angew. Chem. Int. Ed.* **2011**, *50*, 1716.

[51] Y.-X. Zhao, X.-L. Ding, Y.-P. Ma, Z.-C. Wang, S.-G. He, *Theor. Chem. Acc.* **2010**, *127*, 449.

[52] Note, that in certain metal oxide clusters of Groups 5–7 (such as V_3O_8 or $[W_3O_9]^+$), the spin density is distributed among two oxygen atoms, in each case.

[53] Y. X. Zhao, X. N. Wu, Z. C. Wang, S. G. He, X. L. Ding, *Chem. Commun.* **2010**, *46*, 1736.

[54] G. L. Gutsev, L. Andrews, C. W. Bauschlichter, Jr., *Theor. Chem. Acc.* **2003**, *109*, 298.

[55] J. B. Pedley, E. M. Marshall, *J. Phys. Chem. Ref. Data* **1983**, *12*, 967.

[56] a) G. K. Cook, J. M. Mayer, *J. Am. Chem. Soc.* **1994**, *116*, 1855; b) K. Gardner, J. Mayer, *Science* **1995**, *269*, 1849.

[57] a) F. Dong, S. Heinbuch, Y. Xie, J. J. Rocca, E. R. Bernstein, Z.-C. Wang, K. Deng, S.-G. He, *J. Am. Chem. Soc.* **2008**, *130*, 1932; b) Z.-C. Wang, W. Xue, Y.-P. Ma, X.-L. Ding, S.-G. He, F. Dong, S. Heinbuch, J. J. Rocca, E. R. Bernstein, *J. Phys. Chem. A* **2008**, *112*, 5984; c) F. Dong, S. Heinbuch, Y. Xie, E. R. Bernstein, J. J. Rocca, Z.-C. Wang, X.-L. Ding, S.-G. He, *J. Am. Chem. Soc.* **2009**, *131*, 1057; d) Y.-P. Ma, X.-L. Ding, Y.-X. Zhao, S.-G. He, *ChemPhysChem* **2010**, *11*, 1718.

[58] a) G. E. Johnson, R. Mitrić, M. Nössler, E. C. Tyo, V. Bonačić-Koutecký, A. W. Castleman, *J. Am. Chem. Soc.* **2009**, *131*, 5460; b) J.-B. Ma, X.-N. Wu, Y.-X. Zhao, X.-L. Ding, S.-G. He, *Chin. J. Chem. Phys.* **2010**, *23*, 133; c) J.-B. Ma, X.-N. Wu, Y.-X. Zhao, S.-G. He, X.-L. Ding, *Acta Phys. Chim. Sin.* **2010**, *26*, 1761; d) B. Xu, Y.-X. Zhao, X.-N. Li, X.-L. Ding, S.-G. He, *J. Phys. Chem. A* **2011**, *115*, 10245; e) Note, that only the simplest anionic oxo radical, the bare $[O]^{\bullet-}$ ion, exhibits a reactivity towards methane comparable to that found for the cationic systems, that is, $k([O]^{\bullet-} + CH_4) = 8.8 \times 10^{-11}\ cm^3 s^{-1} molecule^{-1}$: A. A. Viggiano, R. A. Morris, T. M. Miller, J. F. Friedman, M. Menedez-Barreto,

J. F. Paulson, H. H. Michels, R. H. Hobbs, J. A. Montgomery, Jr., *J. Chem. Phys.* **1997**, *106*, 8455.

[59] Y.-X. Zhao, J.-Y. Yuan, X.-L. Ding, S.-G. He, W.-J. Zheng, *Phys. Chem. Chem. Phys.* **2011**, *13*, 10084.

[60] a) G. Fu, X. Xu, X. Lu, H. Wan, *J. Am. Chem. Soc.* **2005**, *127*, 3989; b) G. Fu, X. Xu, H. Wan, *Catal. Today* **2006**, *117*, 133.

[61] a) K. M. Jeong, F. Kaufman, *J. Phys. Chem.* **1982**, *86*, 1808; b) W. B. DeMore, *J. Phys. Chem.* **1996**, *100*, 5813; c) A. A. Fokin, P. R. Schreiner, *Chem. Rev.* **2002**, *102*, 1551.

[62] a) K. A. Zemski, D. R. Justes, A. W. Castleman, *J. Phys. Chem. B* **2002**, *106*, 6136; b) R. A. J. O'Hair, G. N. Khairallah, *J. Cluster Sci.* **2004**, *15*, 331; c) K. R. Asmis, A. Fielicke, G. von Helden, G. Meijer in *The Chemical Physics of Solid Surfaces*, *Vol. 12* (Ed.: D. P. Woodruff), Elsevier, **2007**, p. 327.

[63] a) J. H. Lunsford, *Angew. Chem.* **1995**, *107*, 1059; *Angew. Chem. Int. Ed. Engl.* **1995**, *34*, 970; b) J. H. Lunsford, *Catal. Today* **2000**, *63*, 165; c) For a report on the current achievements in the realization of the OCM process, see: S. Jaso, H. R. Godini, H. Arellano-Garcia, M. Omidkhah, G. Wozny, *Chem. Eng. Sci.* **2010**, *65*, 6341.

[64] a) C. R. A. Catlow, S. A. French, A. A. Sokol, J. M. Thomas, *Philos. Trans. R. Soc. London Ser. A* **2005**, *363*, 913; b) K.-P. Dinse, H.-J. Freund, M. Geske, R. Horn, O. Korup, K. Kwapien, S. Mavlyankariev, N. Nilius, T. Risse, J. Sauer, R. Schlögl, U. Zavyalova, 2. Meeting des Scientific Advisory Board von UniCat, Fritz-Haber-Institut Berlin, 27.–28.05. **2010**, Poster A1-3; c) M. Y. Sinev, Z. T. Faltakhova, V. I. Lomonosov, Y. A. Gordienko, *J. Nat. Gas Chem.* **2009**, *18*, 273; d) H. Liu, Y. Wei, J. Caro, H. Wang, *ChemCatChem* **2010**, *2*, 1539; e) U. Zavyalova, M. Holena, R. Schlögl, M. Baerns, *ChemCatChem* **2011**, *3*, 1935.

[65] J. X. Wang, J. H. Lunsford, *J. Phys Chem.* **1986**, *90*, 5883.

[66] T.-J. Yang, J. H. Lunsford, *J. Catal.* **1980**, *63*, 505.

[67] N. W. Cant, C. A. Lukey, P. F. Nelson, R. J. Tyler, *J. Chem. Soc. Chem. Commun.* **1988**, 766.

[68] a) W. Liang, A. T. Bell, M. Head-Gordon, A. K. Chakraborty, *J. Phys. Chem. B* **2004**, *108*, 4362; b) G. I. Panov, K. A. Dubkov, E. V. Starokon, *Catal. Today* **2006**, *117*, 148; c) J. S. Woertink, P. J. Smeets, M. H. Groothaert, M. A. Vance, B. F. Sels, R. A. Schoonheydt, E. I. Solomon, *Proc. Natl. Acad. Sci. USA* **2009**, *106*, 18908; d) E. V. Starokon, M. V. Parfenov, L. V. Pirutko, S. I. Abornev, G. I. Panov, *J. Phys. Chem. C* **2011**, *115*, 2155; e) M. F. Fellah, I. Onal, *Catal. Today* **2011**, *171*, 52; f) P. Vanelderen, R. G. Hadt, P. J. Smeets, E. I. Solomon, R. A. Schoonheydt, B. F. Sels, *J. Catal.* **2011**, *284*, 157.

[69] A. P. Walker, *Catal. Today* **1995**, *26*, 107.

[70] a) M.-H. Baik, M. Newcomb, R. A. Friesner, S. J. Lippard, *Chem. Rev.* **2003**, *103*, 2385; b) R. L. Lieberman, A. C. Rosenzweig, *Nature* **2005**, *434*, 177; c) A. S. Hakemian, A. C. Rosenzweig, *Annu. Rev. Biochem.* **2007**, *76*, 223.

[71] a) R. A. Himes, K. D. Karlin, *Curr. Opin. Chem. Biol.* **2009**, *13*, 119; b) R. Balasubramanian, S. M. Smith, S. Rawat, L. A. Yatsunyk, T. L. Stemmler, A. C. Rosenzweig, *Nature* **2010**, *465*, 115.

[72] a) K. A. Dubkov, N. S. Ovanesyan, A. A. Shteinman, E. V. Starokon, G. I. Panov, *J. Catal.* **2002**, *207*, 341; b) G. Berlier, A. Zecchina, G. Spoto, G. Ricchiardi, S. Bordiga, C. Lamberti, *J. Catal.* **2003**, *215*, 264; c) L. Kiwi-Minsker, D. A. Bulushev, A. Renken, *J. Catal.* **2003**, *219*, 273; d) E. J. M. Hensen, Q. Zhu, M. M. R. M. Hendrix, A. R. Overweg, P. J. Kooyman, M. V. Sychev, R. A. van Santen, *J. Catal.* **2004**, *221*, 560; e) G. D. Pirngruber, P. K. Roy, R. Prins, *J. Catal.* **2007**, *246*, 147.

[73] For a theoretical study, discussing the chemical similarity to biological and biomimetic oxidations, as well as the electronic isomer $Fe^{IV}=O^{2-}$ of the α-oxygen site, see: A. Rosa, G. Ricciardi, E. J. Baerends, *Inorg. Chem.* **2010**, *49*, 3866.

[74] a) K. Otsuka, Y. Wang, *Appl. Catal. A* **2001**, *222*, 145; b) E. Berrier, O. Ovsitser, E. V. Kondratenko, M. Schwidder, W. Grünert, A. Brückner, *J. Catal.* **2007**, *249*, 67.

[75] a) G. Panov, V. Sobolev, K. Dubkov, V. Parmon, N. Ovanesyan, A. Shilov, A. Shteinman, *React. Kinet. Catal. Lett.* **1997**, *61*, 251; b) P. J. Smeets, M. H. Groothaert, R. A. Schoonheydt, *Catal. Today* **2005**, *110*, 303.

[76] K. A. Dubkov, E. A. Paukshtis, G. I. Panov, *Kinet. Catal.* **2001**, *42*, 205.

[77] S. Kameoka, T. Nobukawa, S.-I. Tanaka, S.-I. Ito, K. Tomishige, K. Kunimori, *Phys. Chem. Chem. Phys.* **2003**, *5*, 3328.

[78] B. R. Wood, J. A. Reimer, A. T. Bell, M. T. Janicke, K. C. Ott, *J. Catal.* **2004**, *225*, 300.

[79] a) F. Sastre, V. Vornés, A. Corma, H. García, *J. Am. Chem. Soc.* **2011**, *133*, 17257; b) F. Sastre, V. Vornés, A. Corma, H. García, *Chem. Eur. J.* **2012**, *18*, 1820.

[80] Y. Kim, D. G. Truhlar, M. M. Kreevoy, *J. Am. Chem. Soc.* **1991**, *113*, 7837.

[81] The companion Review by Shaik and co-workers discusses the root cause of the higher reactivity of open-shell abstractor molecules and when this preference ceases to play a role: W. Lai, C. Li, H. Chen, S. Shaik, *Angew. Chem.*, **2012**, *124*, 5652; *Angew. Chem. Int. Ed.*, **2012**, *51*, 5556.